Proceedings of the ASME 2012 Internal Combustion Engine Division Fall Technical Conference
ICEF2012
September 23-26, 2012, Vancouver, BC, Canada

ICEF2012-92045

A REDUCED DIESEL SURROGATE MECHANISM FOR COMPRESSION IGNITION ENGINE APPLICATIONS

Mandhapati Raju
Convergent Science Inc.
Middleton, WI, USA

Mingjie Wang
Convergent Science Inc.
Middleton, WI, USA

P. K. Senecal
Convergent Science Inc.
Middleton, WI, USA

Sibendu Som
Argonne National Laboratory
Argonne, IL, USA

Douglas E. Longman
Argonne National Laboratory
Argonne, IL, USA

ABSTRACT

A skeletal mechanism with 117 species and 472 reactions for a Diesel surrogate i.e., n-heptane, was developed. The detailed mechanism for n-heptane created by Lawrence Livermore National Laboratory (LLNL) was employed as the starting mechanism. The detailed mechanism was then reduced with an enhancement of the Direct Relation Graph (DRG) technique called Parallel DRG-with Error Propagation and Sensitivity Analysis (PDRGEPSA). The reduction was performed for pressures from 20 to 80 atm, equivalence ratios from 0.5 to 2, and an initial temperature range of 600-1200 K, covering the compression ignition (CI) engine conditions. Extensive validations were performed against both 0-D simulations with the detailed mechanism and experimental data for spatially homogeneous systems. In order to perform three-dimensional turbulent spray-combustion and engine simulations, the mechanism was integrated with the multi-zone model in the CONVERGE CFD software to accelerate the calculation of detailed chemical kinetics. The Engine Combustion Network (ECN) data from Sandia National Laboratory was used for validation purposes along with single-cylinder Caterpillar engine data. The skeletal mechanism was able to predict various combustion characteristics accurately such as ignition delay and flame lift-off length (LOL) under different ambient conditions. The performance of the multi-zone solver with respect to the full cell-by-cell chemistry solver (SAGE) is compared for the Caterpillar engine simulation and a good match is obtained with significant speed-up of computational time for the multi-zone solver.

INTRODUCTION

It is a formidable challenge to run detailed kinetic mechanisms containing hundreds or thousands of species in a three-dimensional Computational Fluid Dynamics (CFD) based engine simulation code. The computational cost of chemistry scales by the third power of the number of species in the worst case when factorizing the Jacobian [1]. Hence, it is necessary to reduce the mechanisms for practical internal combustion engine (ICE) simulations. In addition, three-dimensional combustion simulations are computationally expensive even when smaller mechanisms are used. Typically three-dimensional simulations involve invoking the chemistry solver for up to a few million CFD cells. Multi-zone modeling can significantly enhance the computational speed by invoking the chemistry solver on only a relatively small number of zones. A combination of multi-zone chemistry and reduced mechanisms can significantly decrease the computational time of three-dimensional combustion simulations.

Skeletal mechanism reduction involves removing species and reactions from the detailed mechanism which are deemed negligible to important phenomena over the range of conditions of interest (e.g. pressure, temperature, and equivalence ratio). Classical skeletal reduction methods include sensitivity analysis [2-4] and principal component analysis [5]. Other important

 Copyright © 2012 by ASME

methods include lumping [6-8], genetic algorithms [9, 10], optimization [11-13], and adaptive reduction approaches [14-18].

The Directed Relation Graph (DRG) method was originally proposed by Lu and Law [19]. A directed relation graph is used to map the coupling of species. Unimportant species are identified and removed based on selected target species and an acceptable error threshold. There have been several enhancements to this DRG method. DRG-Aided Sensitivity Analysis (DRGASA) [20, 21] performs sensitivity analysis on species not removed by DRG to further reduce the mechanism. DRG with Error Propagation (DRGEP) [22] considers the propagation of error due to species removal down reaction pathways. A path flux analysis [23] was recently presented that uses production and consumption fluxes to identify important reaction pathways. DRG with Error Propagation and Sensitivity Analysis (DRGEPSA) integrates the major aspects of DRGEP and DRGASA. It has been shown that this combined approach overcomes the weaknesses of the two individual methods [24]. An algorithm of DRG with expert knowledge (DRG-X) [25] has also been employed as the first step to eliminate unimportant species and reactions. DRG-X alleviates limitations of the original DRG and allows non-uniform error tolerances (specified by an expert) for different species and heat release, while it features similar low reduction cost as that of DRG. Recently, DRG-X has been combined with DRGASA and isomer lumping to reduce detailed reaction mechanisms for diesel and biodiesel fuel surrogates [26-27].

Skeletal mechanism generation using DRGEPSA is a time consuming process. For detailed mechanisms containing thousands of species, DRGEPSA would typically take a few days to generate a skeletal mechanism. The core of the skeletal mechanism reduction algorithms consists of running zero-dimensional auto-ignition delay simulations for a range of operating conditions. As the size of the detailed mechanism increases, the CPU time of the auto-ignition simulations also increases. This paper presents parallelization of the skeletal mechanism generation on distributed machines to reduce the computational time significantly. Since the auto-ignition simulations are all decoupled, good speed-up of the parallel mechanism generation code is expected. The mechanism reduction is implemented into the CONVERGE CFD solver [28, 29]. The SAGE chemistry solver, which is part of CONVERGE, is used for the auto-ignition simulations.

For engine combustion simulations, the multi-zone modeling concept is used to significantly reduce the computational time. Aceves et al. [30] used a sequential multi-zone approach for Homogenous Charge Compression Ignition (HCCI) simulations. In their approach, fluid mechanics is solved until the start of combustion. Then the entire domain is split into many zones based on the local temperature. Chemistry is then solved on each of the zones. Inter-zone mass transfer and heat transfer is completely neglected. The results show a good prediction of maximum pressure, burn duration and combustion efficiency. However, there were discrepancies in the prediction of HC and CO emissions.

Flowers et al. [31] and Babajimopoulos et al. [32] extended this method to couple the zone-based chemistry solution and the cell-based transport solution via an interactive mapping technique. The cells are divided based on the cell temperature and the cell equivalence ratio. The zonal solution is then remapped to the individual cells based on an empirically defined "ch" value for each cell. This method has been successfully demonstrated for HCCI and PCCI (Premixed Charge Compression Ignition) problems [32-33]. Liang et al. [34] presented a dynamic multi-zone (DMZ) partitioning scheme, which dynamically determines the optimal number of zones using a rigorous data-clustering technique. In addition, they report a different remapping strategy for mapping the zonal solution on to the individual cells in the zone. The zoning methodology of Babajimopoulos et al. [32] has been recently improved by Raju et al. [35] to include both a variable binning strategy and an n-dimensional binning strategy. They report better performance of the multi-zone solver using three binning variables for dual fuel injection cases.

The rest of this paper is outlined as follows. Firstly, the parallel version of the DRGEPSA reduction algorithm is described. In this paper, n-heptane is used as a surrogate for Diesel fuel. The detailed n-heptane mechanism is reduced using the parallel version of DRGEPSA. Secondly, a brief description of the multi-zone chemistry solver is presented. The results for 0D and 3D constant volume simulations are then compared with experiments. Ignition delay times are compared with the shock tube experiments [36] and rapid compression machine experiments [37] for n-heptane fuel. Experimental data to use for comparison for 3D constant volume studies are obtained from Sandia National Laboratories through the Engine Combustion Network (ECN) [38-40]. Three dimensional simulation of a single cylinder Caterpillar engine is presented and the computational efficiency of the multi-zone solver is demonstrated for the reduced mechanism.

PARALLEL MECHANISM REDUCTION ALGORITHM

The DRGEPSA algorithm essentially consists of two phases: (1) DRGEP and (2) Sensitivity analysis (SA). The details of DRGEP and SA are explained in detail in [24-27]. Only the outline of the DRGEPSA algorithm is presented here with emphasis on the parallelization scheme. Figure 1 shows the flow chart of the DRGEPSA algorithm. First, a number of auto-ignition simulations are set up for the given range of initial temperature, pressure and equivalence ratio conditions. For each case, a set of sample points are selected along the integration curve at intervals of a 10 K temperature difference. For each sample point, the DRGEP coefficients are calculated based on a set of target species. Once the OIC's (Overall Interaction Coefficients) are calculated, different cut-off tolerances for OIC's are chosen and a skeletal mechanism is

Copyright © 2012 by ASME

generated for each cut-off value. For each of the resulting skeletal mechanisms generated, auto-ignition simulations are performed and the maximum error in the ignition time delay values as compared to the detailed mechanism is calculated. An optimal mechanism is thus chosen as the smallest mechanism whose error in the ignition delay is within the tolerance limit set by the user.

Once the optimal mechanism is obtained from the DRGEP step, sensitivity analysis is performed to further reduce the size of the mechanism. In the sensitivity analysis phase, the OIC values of the species in the skeletal mechanism are arranged in ascending order and a fixed fraction of the species from the top of the list is chosen for sensitivity analysis. This list of species is referred to as the limbo species. The error induced by each of the species is calculated by removing this species from the DRGEP generated skeletal mechanism. The error in the ignition delay is then calculated for the resulting skeletal mechanism. This error is an indication of the sensitivity of the species to the prediction of ignition delay time. Now the species are arranged in ascending order based on this error. The next step is to determine the optimal skeletal mechanism that would result from the sensitivity analysis. This is done by removing the species identified from the top of the list one by one from the DRGEP generated mechanism until the error generated by the resulting skeletal mechanism exceeds the user set tolerance for ignition delay. Thus the optimal skeletal mechanism is obtained. All of the steps in the algorithm are executed sequentially.

To reduce the computation time of the mechanism reduction algorithm, it can be parallelized on a cluster of computer nodes. The core of the parallelization occurs in splitting the zero-dimensional auto-ignition delay simulations amongst the different processors. This is accomplished with MPI programming. The zero-dimensional cases are set up based on the range of operating conditions for which a skeletal mechanism is being requested. Typically, a range of different initial temperatures, pressures and fuel equivalence ratios are chosen. This would lead to a minimum of 8 (2x2x2) cases. The maximum number of cases could be as high as a few hundred. If a higher number of cases is chosen, the computational time would proportionately increase. Since all of the auto-ignition simulations are decoupled, they can be easily distributed amongst the processors. Ideally, the maximum speed-up in the wall clock time can be obtained by choosing as many numbers of processors as the number of zero-dimensional cases chosen. However, it should be noted that some of the auto-ignition cases will run faster and some of them will run slower depending on the operating conditions. In addition, there is an overhead in parallel MPI communications due to MPI barrier synchronization. Hence, an ideal speed-up is not possible to achieve. But nevertheless, the gain in the wall clock time is quite significant.

Figure 1 shows the parallel DRGEPSA algorithm. First the auto-ignition cases for the detailed mechanism are split amongst the different processors. The best parallelization is obtained when the number of cases is an integer multiple of the number of processors chosen (assuming each case takes the same CPU time). This will ensure each processor to run only a single zero-dimensional case. Once all the processors have completed all the cases assigned to it, the ignition delay values of all the simulations are broadcasted to all the processors. Each processor will generate its own data of sample points from the zero-dimensional cases assigned to it and write it to a common data file on the hard disk. Next the DRGEP algorithm is applied on each of the sample points. The sample points are read in from the data file on the hard disk by all the processors and are distributed equally (or nearly equally) amongst the different processors.

Once the DRGEP step is done, the OIC values are calculated on each of the processors. The global maximum of the OIC values on all the processors is obtained using the MPI_ALLREDUCE operation. Each processor will now have the global OIC values. Based on the global OIC values, an optimal mechanism is generated as described in the previous section. Note that with each new skeletal mechanism generated during this search phase, zero-dimensional cases are run with that skeletal mechanism. This is done in parallel using the procedure previously described. The same procedure is continued for the sensitivity analysis phase. Whenever zero-dimensional simulations have to be performed, they are computed in parallel. Thus it is observed that each step of the skeletal mechanism reduction can be performed in parallel due to the decoupled nature of the simulations. A following section describes the speed-up obtained for the mechanism reduction simulations during parallel computation.

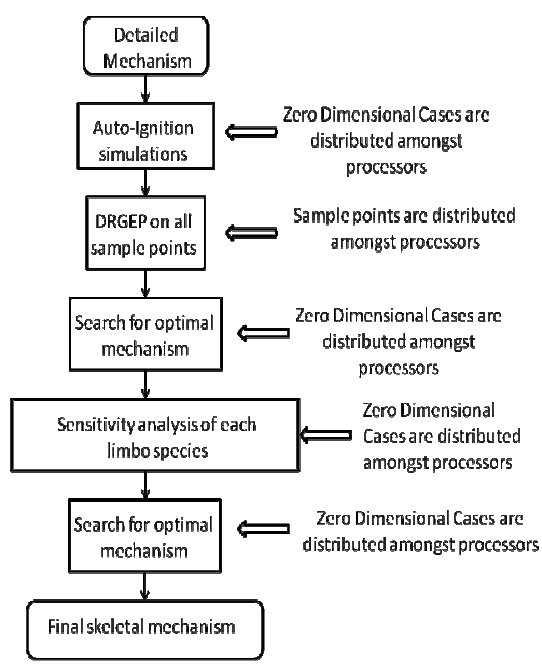

Figure 1: Flow chart of the parallel DRGEPSA algorithm

Copyright © 2012 by ASME

Once the DRGEP step is done, the OIC values are calculated on each of the processors. The global maximum of the OIC values on all the processors is obtained using the MPI_ALLREDUCE operation. Each processor will now have the global OIC values. Based on the global OIC values, an optimal mechanism is generated as described in the previous section. Note that with each new skeletal mechanism generated during this search phase, zero-dimensional cases are run with that skeletal mechanism. This is done in parallel using the procedure previously described. The same procedure is continued for the sensitivity analysis phase. Whenever zero-dimensional simulations have to be performed, they are computed in parallel. Thus it is observed that each step of the skeletal mechanism reduction can be performed in parallel due to the decoupled nature of the simulations. The next section described the speed-up obtained for the mechanism reduction simulations during parallel computation.

MULTI-ZONE CHEMISTRY SOLVER

The multi-zone chemistry solver is coupled to the CONVERGE CFD solver [28-29]. CONVERGE uses a modified cut-cell Cartesian technique and includes state-of-the-art numerical methods and sub-models for simulating the complex physical and chemical processes that occur in engines. These include models for spray injection, atomization and breakup, turbulence, droplet collision and coalescence, evaporation, heat-transfer etc. The gas-phase flow field is described by using the Favre-Averaged Navier-Stokes equations in conjunction with the RNG k-ε turbulence model, which includes source terms for the effects of dispersed phase on gas-phase turbulence. These equations are solved by using a finite volume solver. CONVERGE has an integrated chemistry solver, referred to as SAGE, which performs the detailed chemistry calculations on each grid cell. In contrary to the detailed chemistry solver (SAGE), the multi-zone model solves chemistry only on a relatively small number of zones.

Figure 2 shows the schematic of the multi-zone solver. At each discrete time t, the cells are grouped in zones based on the thermodynamic state of the cell. In a two-dimensional zoning strategy, the zoning is done based on two variables, the temperature and the equivalence ratio of the cells. For each zone, the average temperature, pressure and the composition are determined to specify the thermodynamic state of the mixture in that zone. The SAGE chemistry solver is invoked on each zone. The zonal solution is then remapped onto the individual cells. The zoning strategy and remapping strategy are discussed in detail in Ref. [35].

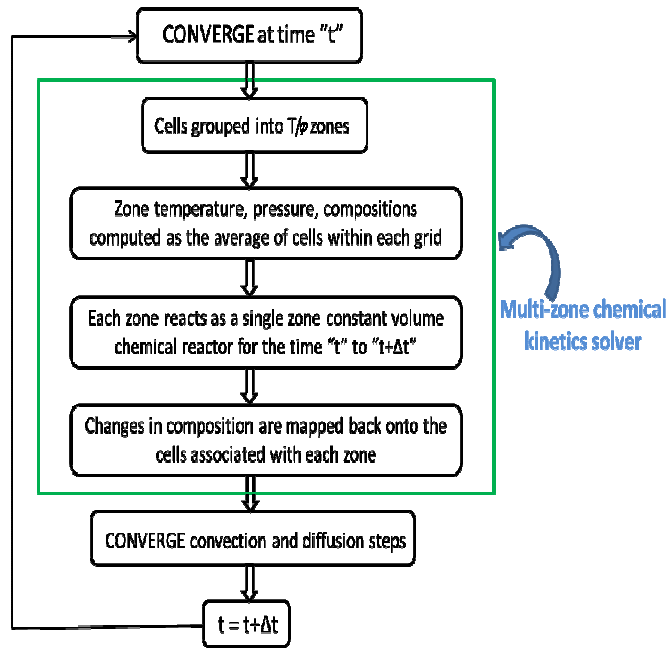

Figure 2: Schematic of the two-dimensional multi-zone algorithm in CONVERGE

RESULTS AND DISCUSSION

(a) Mechanism Reduction

First, the n-heptane detailed mechanism consisting of 561 species and 2539 reactions developed by Lawrence Livermore National Laboratory is reduced using PDRGEPSA. The temperature range is chosen as 600-1200K, the pressure range is chosen as 20-80 bar and the equivalence ratio is chosen as 0.5-2.0. A total of 64 cases are taken in this range. The tolerance limit was chosen as 25% and the target species are chosen as n-heptane and OH. A skeletal mechanism consisting of 117 species and 472 reactions was obtained as a result of the reduction process. As a demonstration of the parallel performance, the reduction process was repeated using different numbers of processors. The resultant skeletal mechanism is unaffected by the choice of the number of processors but the computational time varies. Figure 3 shows the Wall clock time in hours on different numbers of processors. The time is indicated on the top of the bar and the relative speed-up with respect to the single processor is reported in the brackets. As shown in Figure 3, the computation time taken for the reduction process decreases with the increase in the number of the processors. On 64 processors, a speed of around 19 times is observed. Thus, there is a significant reduction in wall-clock time for generating skeletal mechanisms using parallel computations.

Copyright © 2012 by ASME

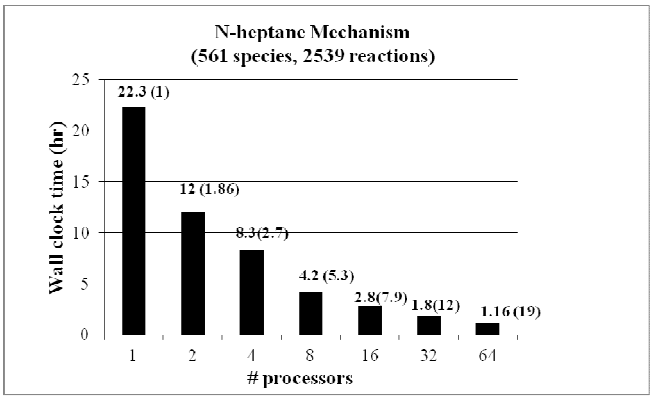

Figure 3: Comparison of CPU times on different numbers of processors for an n-heptane mechanism

(b) Comparison with 0D experiments

The performance of the skeletal mechanism is evaluated with respect to both the detailed mechanism and experimental results for constant volume zero-dimensional homogenous combustion. Ignition delay data is available from experiments [36-37]. The comparison is done for three equivalence ratios, 0.5, 1.0, and 2.0. The experimental data is available at three different pressures, 3 bar, 13.5 bar and 42 bar for a stoichiometric mixture, and at two different pressures (13.5 bar and 42 bar) at equivalence ratios of 0.5 and 2.0. The constant volume zero-dimensional simulations were performed using CONVERGE's zero-dimensional solver. Figure 4 shows the comparison of the ignition delay from experiments and the ignition delay predictions using the detailed and skeletal mechanisms. Experimental data is represented with symbols, the detailed mechanism is shown with solid lines, and the skeletal mechanism is shown using dashed lines. There is a slight deviation in the predictions using the skeletal mechanism as compared to the detailed mechanism. Given the uncertainty in the experimental data and detailed mechanism prediction, the skeletal mechanism gives a reasonably good prediction.

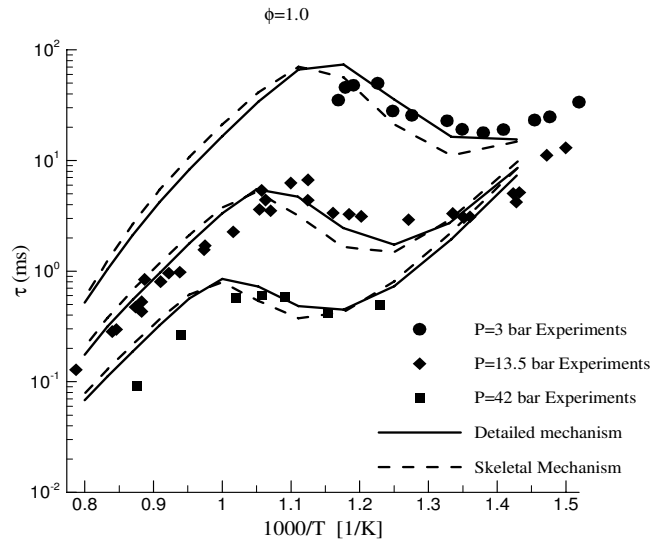

Figure 4: Comparison of ignition delay of n-heptane for an equivalence ratio of 1.0

Figures 5 and 6 show similar comparisons between the experiments, detailed, and skeletal mechanisms for equivalence ratios of 0.5 and 2.0, respectively. The skeletal mechanism is found to give a reasonably good prediction as compared to the detailed mechanism and the experimental data.

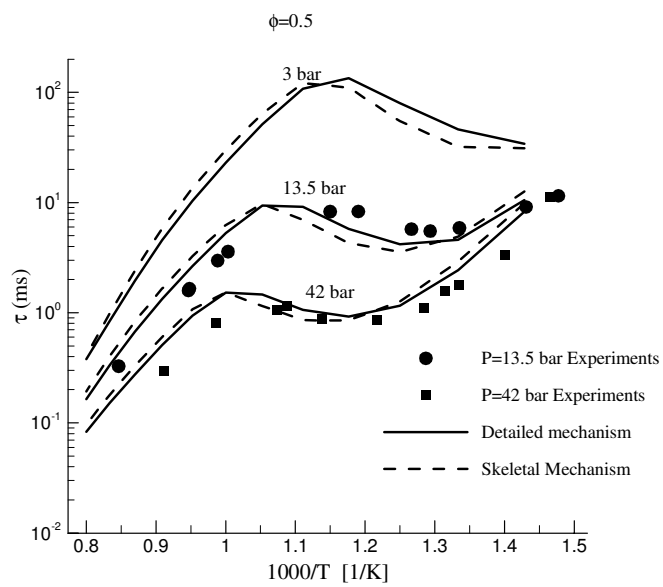

Figure 5: Comparison of ignition delay of n-heptane for an equivalence ratio of 0.5

Copyright © 2012 by ASME

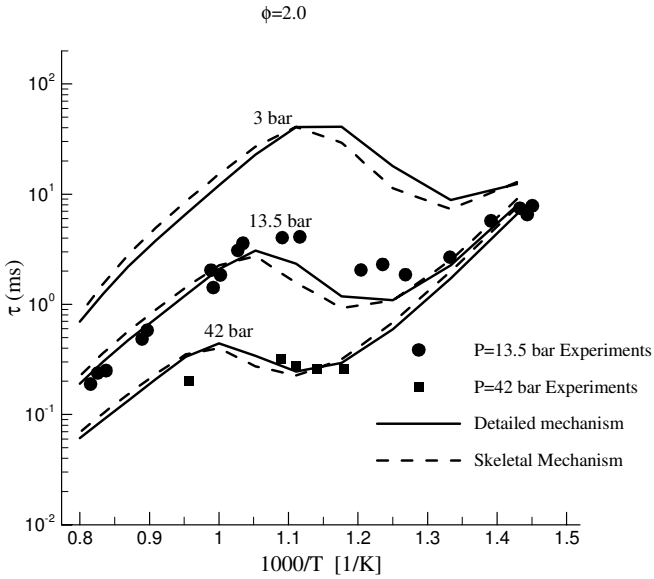

Figure 6: Comparison of ignition delay of n-heptane for an equivalence ratio of 2.0

(c) Comparison with 3D constant volume experiments

This section presents validation of the 117 species, 472 reaction n-heptane skeletal mechanism against 3D constant volume spray-combustion data from Sandia National Laboratory [38-40]. A brief overview of the experiments is first provided. These experiments were conducted in a constant-volume, quiescent, pre-burn-type combustion vessel to generate high-temperature and high-pressure gases to simulate the thermodynamic conditions obtained in an engine. A premixed combustible mixture is spark-ignited, which burns to completion. The combustion products cool over a long time due to heat transfer to the vessel walls resulting in a decrease in vessel pressure. Once the desired pressure and temperature are reached, the diesel fuel injector is triggered and fuel injection occurs. The ambient conditions for the experimental study are noted in Table 1. The measured rate of injection (ROI) is a top-hot profile. Advanced optical diagnostics are used to obtain the liquid and vapor penetration versus time, liquid length, ignition delay, and flame lift-off length (LOL) etc., to validate the spray and combustion models. The definitions used for liquid length, vapor penetration, ignition delay, and LOL in the simulations are also noted (Table 2).

Table 1: Range of conditions for spray-combustion experiments at Sandia National Laboratory for n-heptane

Fuel Conditions	**n-Heptane**
Ambient temperature (K)	800–1300
Ambient density (kg/m^3)	14.8
Composition	Non-combusting: 0% O_2 Combusting: 10–21% O_2
Injection pressure (bar)	1,500
Fuel injection temperature (K)	373
Nozzle diameter (μm)	100
Duration of injection (ms)	6.8
Total mass injected (mg) Top-hat profile	17.8

Table 2 – Various definitions used for different parameters of interest

Parameter	**Definition**
Liquid length	Axial distance encompassing 97% of injected liquid fuel mass
Vapor penetration	Maximum distance from the injector where the fuel mass fraction is 5% of the peak value
Ignition delay	Ignition is said to occur when T is ≥2000 K in any cell
Flame LOL	Farthest upstream axial location of the T = 2000 K iso-contour

Extensive validations of spray parameters have been performed to ensure that the fuel-air mixing is accurately captured by the simulations. Some sample results are shown in Figure 7 which compares liquid spray and vapor penetration, as well as mixture fraction between experiments and simulations. In general, the parameters are well captured by the simulations under the conditions investigated. Validations against various other ambient conditions have also been performed (not shown here), and the spray simulations are able to capture the experimental trends well.

Copyright © 2012 by ASME

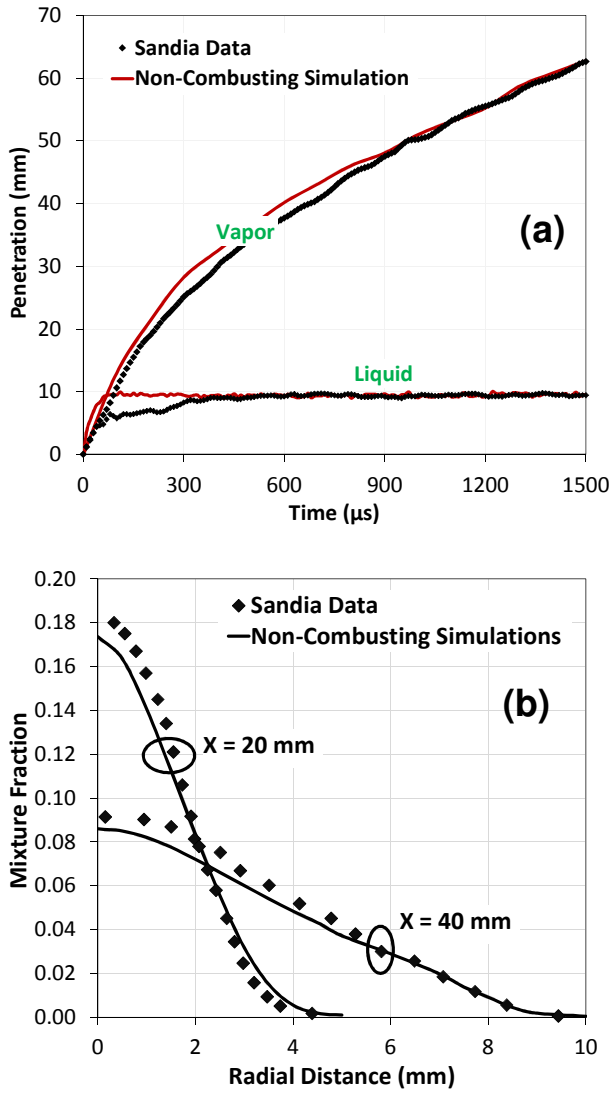

Figure 7: Comparison of (a) liquid and vapor penetration, (b) mixture fraction between experiments from Sandia [38] and simulations using CONVERGE under non-combusting conditions described in Table 1 at an ambient temperature of 1000 K

Following validation under non-combustion conditions, Figures 8 and 9 compare the predictions by the 117 species mechanism against data from Sandia. These simulations are performed using the multi-zone solver described in section 3. The bin sizes for temperature and equivalence ratio are 5 K and 0.05 respectively. Simulations performed using a typical mechanism currently used for 3D CFD simulations is also shown which consists of 68 species and 283 reactions [41]. These simulations are performed using SAGE, and do not incorporate the multi-zone solver [42]. The main objective is to demonstrate the fidelity and computational-time benefits of using a large mechanism (117 species, 472 species) in conjunction with a multi-zone solver compared to a standard approach in the literature involving a smaller mechanism without the multi-zone solver. Simulations using both the approaches are performed with a base grid size of 4 mm resulting in a minimum grid size of 0.25 mm due to four levels of fixed embedding and adaptive meshing to the velocity and temperature fields.

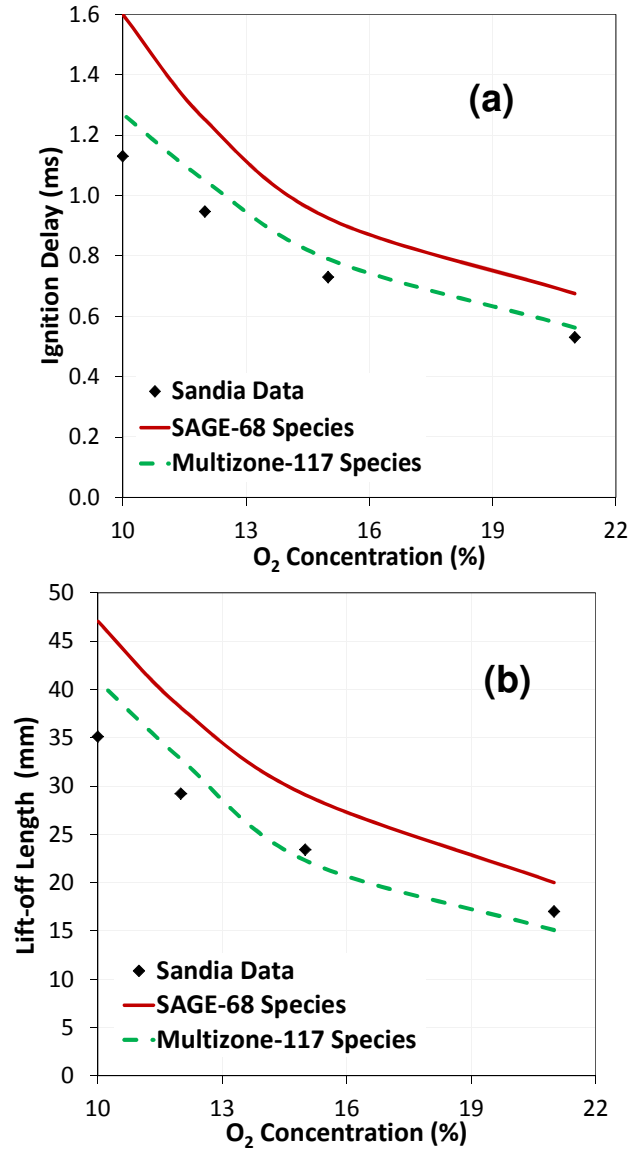

Figure 8: Comparison of (a) ignition delay, (b) flame LOL at different ambient oxygen concentrations between experiments from Sandia [38] and simulations using CONVERGE under combusting conditions described in Table 1 at an ambient temperature of 1000 K, and ambient density of 14.8 kg/m^3.

An increase in the ambient oxygen concentration results in the decrease of both ignition delay and flame LOL. This is due to the fact that the flame reactivity (or the Damköhler number) is enhanced. Simulations with both mechanisms can capture this trend qualitatively well. However, the 117 species mechanism also captures the quantitative values very well, especially at

Copyright © 2012 by ASME

higher oxygen concentrations. The 68 species mechanism tends to over predict both ignition delay and flame LOL at all oxygen concentrations compared to both the 117 species mechanism and the experimental data from Sandia.

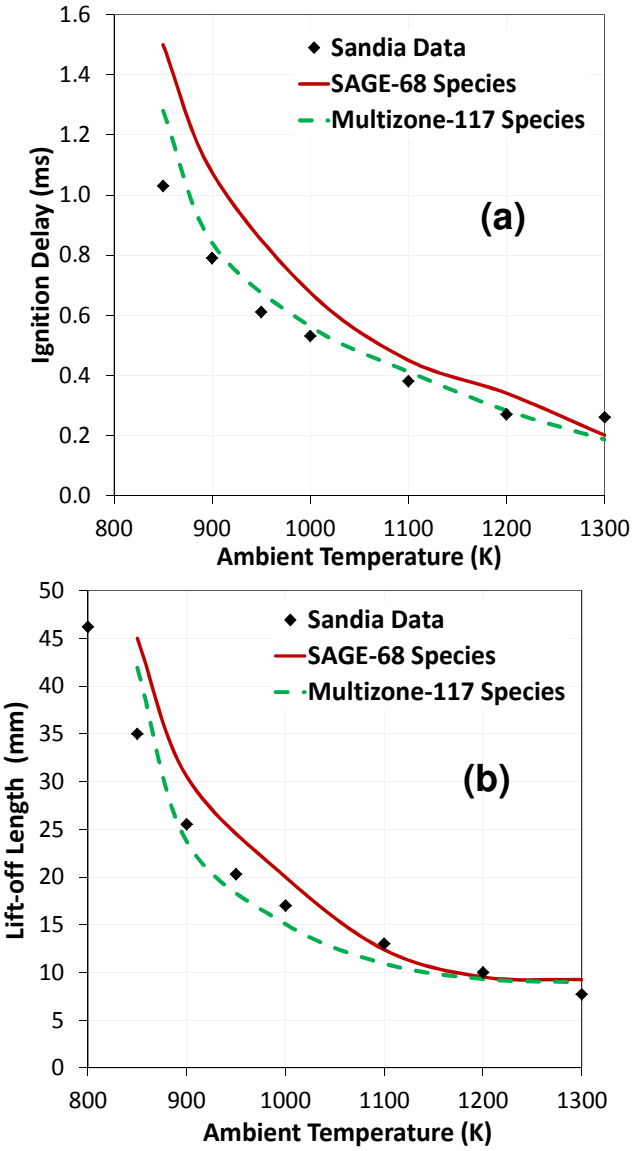

Figure 9: Comparison of (a) ignition delay, (b) flame LOL at different ambient temperatures between experiments from Sandia [38] and simulations using CONVERGE under combusting conditions described in Table 1 at an ambient Oxygen concentration of 21%, and ambient density of 14.8 kg/m^3.

An increase in the ambient temperature results in the decrease of both ignition delay and flame LOL. This is due to the fact that the flame reactivity is enhanced with the increase in ambient temperature. Simulations with both mechanisms can capture this trend qualitatively well. However, the 117 species mechanism also captures the quantitative values very well, especially in the temperature range of 900 – 1200 K. The 68 species mechanism in general tends to overestimate both ignition delay and flame LOL compared to the 117 species mechanism, especially at ambient temperatures less than 1100 K.

Wall-clock times for the 117 species mechanism with the multi-zone solver and 68 species mechanism with the SAGE solver on 24 processors are tabulated in Table 3. These simulations were stopped after 2 ms from the start of injection (SOI) to save computational resources. In general, at both temperatures a factor of (approximately) three speed-up is observed. Cleary, the accuracy of ignition delay and flame LOL predictions (cf. Figs. 8 and 9) with the detailed 117 species mechanism and the speed-up obtained by implementing the multi-zone solver, can facilitate high-fidelity 3D turbulent spray combustion simulations in a computationally tractable manner.

Table 3 – Comparison of wall-clock times for 117 species mechanism with the multi-zone solver, and 68 species mechanism with the SAGE solver.

Temperature (K)	Multi-zone - 117 species	SAGE – 68 species
	Wall-clock time (hours)	Wall-clock time (hours)
850	39	118
1000	48	157

The accuracy and wall-clock times for the 117 species mechanism with the multi-zone solver are compared against that of the SAGE solver on 24 processors in Table 4. These simulations were stopped after 2 ms from SOI to save computational resources. Under both the ambient temperature conditions, the SAGE solver predictions are closer to the experimental data compared to the multi-zone solver. However, the improvement in ignition delay predictions is less than ± 10% while using the SAGE solver. As expected, the wall-clock times are significantly greater for the SAGE simulations. In fact, under all conditions investigated a speed-up of more than seven is observed with the multi-zone solver compared to SAGE. Considering the accuracy and computational cost, our results indicate that the multi-zone simulations can be applied for 3D turbulent spray combustion simulations since it facilitates implementation of higher fidelity detailed chemical-kinetic models. Future studies will focus on further reducing the discrepancies between SAGE and the multi-zone solver results by performing three dimensional binning and varying the bin sizes.

Copyright © 2012 by ASME

Table 4 – Comparison of ignition delay results between 117 species mechanism with the multi-zone and SAGE solvers against experimental data from Sandia [38]. The wall-clock times for both multi-zone and SAGE solvers are also shown.

Temperature (K)	Data	Multi-zone		SAGE	
	Ignition Delay (ms)	Ignition Delay (ms)	Wall-clock time (hours)	Ignition Delay (ms)	Wall-clock time (hours)
850	1.03	1.25	39	1.22	212
1000	0.53	0.56	48	0.51	362

Table 5 –Engine specifications and operating conditions

Bore x stroke (mm)	137.2 x 165.1
Compression ratio	16:1
Engine speed (rev/min)	1600
Start of injection (^{o}ATDC)	-9
Temperature at IVC(K)	355
Pressure at IVC (bar)	2
EGR (% by mass)	0%

(c) Three dimensional engine combustion simulations

Having gained confidence in the performance of the skeletal mechanism, it is used in the simulation of a Diesel engine. However, it is to be noted that even with a reduced mechanism, three dimensional combustion simulations are computationally expensive. Hence, the multi-zone chemistry solver is used. The performance of the multi-zone solver is compared with that of the SAGE solver. A Caterpillar Single-Cylinder Oil Test Engine (SCOTE) operating in a CI mode is simulated using the reduced mechanism. The engine specifications and modeled operating conditions are shown in Table 5. A 60-degree sector mesh is used in the simulations. Diesel spray is injected at -9 ATDC (After Top Dead Center) for a duration of 21 crank degrees. N-heptane is used as a surrogate for Diesel fuel. A base grid size of 1.4 mm is used with a minimum cell size of 0.35 mm due to velocity and temperature adaptive mesh refinement. The skeletal mechanism generated in this work is used in simulating Diesel combustion. A bin size of 5 K is used for temperature and a bin size of 0.05 is used for the equivalence ratio. Figures 10 and 11 show the comparison of the performance of SAGE and the multi-zone solver. Figure 10 shows the average pressure, average temperature and maximum temperature profiles in the cylinder as functions of crank angle. The results show that the multi-zone simulations match quite closely to the SAGE simulations. Note that the distribution of the fuel is highly stratified in this case and yet there is a good match between SAGE and multi-zone. Figure 11 shows the comparison of the heat release rate and the species mass. The heat release rate of the multi-zone simulations is lower compared to that of the SAGE simulations at the start of ignition. The multi-zone simulations exhibit slightly earlier ignition but a lower peak in heat release rate compared to SAGE. All of the species masses are well predicted by the multi-zone simulations. The multi-zone simulation took 22 hours of wall clock time and SAGE took 240 hours of wall clock time. Multi-zone gives a speed-up of around 11 times compared to solving chemistry in every computational cell with SAGE.

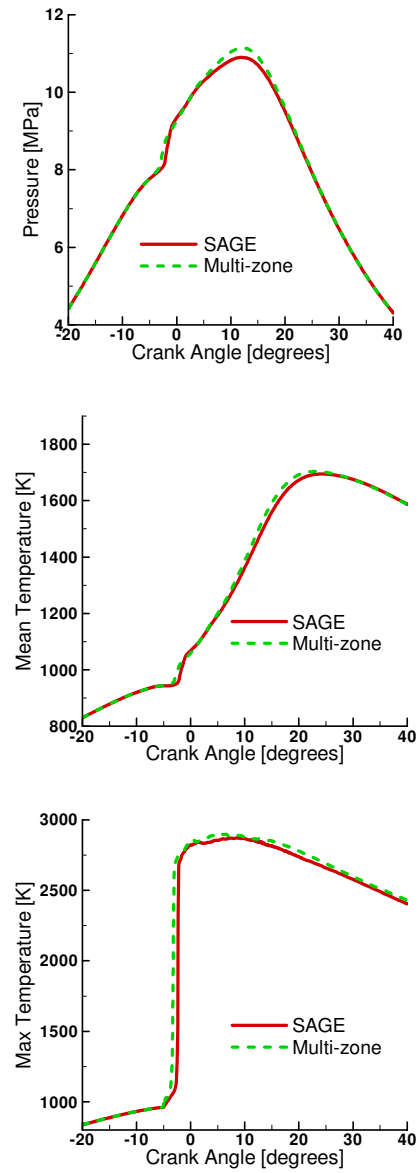

Figure 10: Comparison of average pressure, average temperature and maximum temperature for Multi-zone and SAGE

Copyright © 2012 by ASME

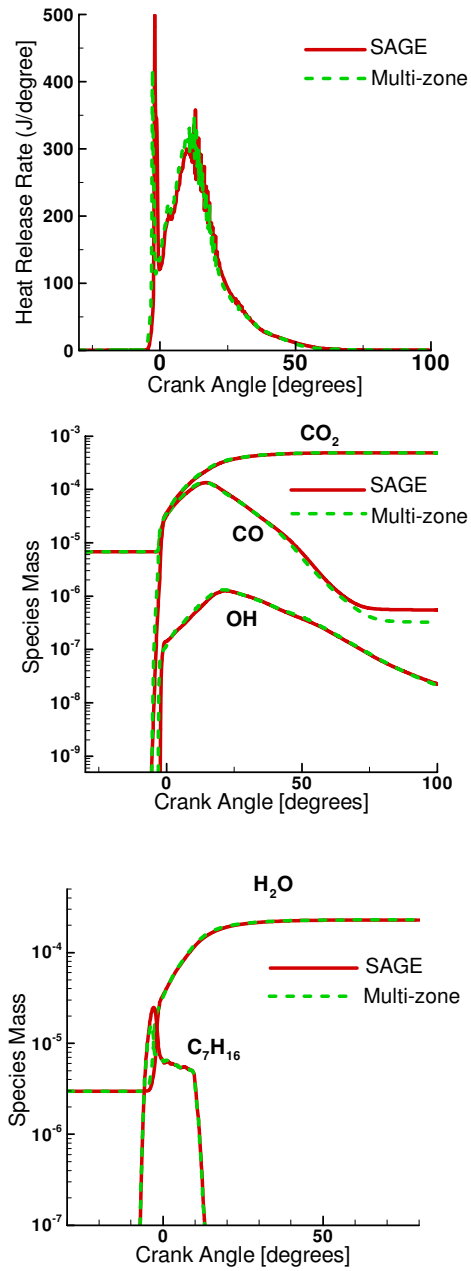

Figure 11: Comparison of heat release rate and species mass for Multi-zone and SAGE

CONCLUSION

A three-dimensional compression ignition internal combustion engine simulation is performed using a reduced diesel surrogate mechanism and the multi-zone chemistry model. A reduced diesel surrogate mechanism consisting of 117 species and 472 reactions is generated under engine conditions using the parallel DRGEPSA reduction tool. The performance of the reduced mechanism is demonstrated using 0D and 3D constant volume simulations. The ignition delay times for 0D simulations compare well with experiments. The three dimensional constant volume simulations are compared with 3D constant volume spray-combustion data from Sandia National Laboratory obtained through the ECN. The various combustion characteristics such as ignition delay and flame lift-off length (LOL) under different ambient conditions are captured well by the skeletal mechanism running with a multi-zone model. The use of the multi-zone model gives a speed-up of around 5-7 times compared to SAGE. A typical three dimensional Diesel engine simulation is performed using the skeletal mechanism. The performance of the multi-zone model is compared with SAGE. The multi-zone model is able to capture cylinder pressure, temperature, heat release and even the species profiles as compared to SAGE. A speed-up of around 11 times is obtained using the multi-zone solver. The use of the reduced mechanism coupled with a multi-zone chemistry solver can significantly reduce the computational time while retaining a reasonable level of accuracy.

ACKNOWLEDGMENTS

The submitted manuscript has been created in collaboration with UChicago Argonne, LLC, operator of Argonne National Laboratory (Argonne). Argonne, a U.S. Department of Energy Office of Science laboratory, is operated under Contract No. DE-AC02-06CH11357. The U.S. Government retains for itself, and others acting on its behalf, a paid-up, nonexclusive, irrevocable worldwide license in said article to reproduce, prepare derivative works, distribute copies to the public, and perform publicly and display publicly, by or on behalf of the Government.

The implementation of the multi-zone solver into CONVERGE was done in collaboration with Lawrence Livermore National Laboratory.

The authors would like to acknowledge the staff of Convergent Science, Inc. for their support and encouragement.

REFERENCES

[1] Lu, T., Law, C.K., 2009, "Toward accommodating realistic fuel chemistry in large-scale computations," Progress in Energy and Combustion Science, Vol. 35, No. 2, pp. 192-215.

[2] Rabitz, H., Kramer, M., Dacol, D., 1983, "Sensitivity Analysis in Chemical Kinetics," Ann. Rev. Phys. Chem., Vol. 34, pp. 419–461.

[3] Turányi, T., 1990, "Sensitivity analysis of complex kinetic systems. Tools and applications," J. Math. Chem., Vol. 5, No. 3, pp. 203–248.

[4] Turányi, T., 1990, "Reduction of large chemical mechanism," New J. Chem. Vol. 14, No. 11, pp. 795–803.

 Copyright © 2012 by ASME

[5] Vajda, S., Valko, P., Turányi, T., 1985, "Principal component analysis of kinetic models," Int. J. Chem. Kinetics, Vol. 17, No. 1, pp. 55–81.

[6] Li, G., Rabitz, H., 1989, "A general analysis of exact lumping in chemical kinetics," Chem. Eng. Sci. Vol. 44, No. 6, pp. 1413–1430.

[7] Huang, H., Fairweather, M., Griffiths, J.F., Tomlin, A.S., Brad, R.B., "A systematic lumping approach for the reduction of comprehensive kinetic models", Proc. Combust. Inst., Vol. 30, pp. 1309-1316.

[8] Pepiot-Desjardins, P., Pitsch, H., 2008, "An automatic chemical lumping method for the reduction of large chemical kinetic mechanisms," Combust. Theory Model. Vol. 12, No. 6, pp. 1089–1108.

[9] K. Edwards, T. Edgar, V. Manousiouthakis, Comput. Chem. Eng. 22 (1–2) (1998) 239–246.

[10] Elliott, L., Ingham, D., Kyne, A., Mera, N., Pourkashanian, M., Wilson, C., 2004, "Genetic algorithms for optimisation of chemical kinetics reaction mechanisms," Prog. Energy Combust. Sci., Vol. 30, No. 3, pp. 297–328.

[11] Bhattacharjee, B., Schwer, D., Barton, P.I., Green, W., 2003, "Optimally-reduced kinetic models: reaction elimination in large-scale kinetic mechanisms," Combust. Flame, Vol. 135 No. 3, pp. 191–208.

[12] O.O. Oluwole, B. Bhattacharjee, J. Tolsma, P.I. Barton, W. Green, 2006, "Rigorous valid ranges for optimally reduced kinetic models," Combust. Flame, Vol. 146, No. 1–2, pp.348-365.

[13] A. Mitsos, G. Oxberry, P.I. Barton, W. Green, 2008, "Optimal automatic reaction and species elimination in kinetic mechanisms," Combust. Flame, Vol. 155, pp. 118–132.

[14] Løvås, T., Mauss, F., Hasse, C. and Peters, N. (2002), "Development of Adaptive Kinetics for Application in Combustion Systems," Proc. Comb. Inst. Vol. 29, pp. 1387-1393.

[15] D. Schwer, P. Lu, W. Green, 2003, "An adaptive chemistry approach to modeling complex kinetics in reacting flows," Combust. Flame, Vol. 133, No. 4, pp. 451–465.

[16] I. Banerjee, M. Ierapetritou, 2006, "An adaptive reduction scheme to model reactive flow," Combust. Flame, Vol. 144, No. 3, pp. 619–633.

[17] O.O. Oluwole, P.I. Barton, W. Green, 2007, "Obtaining accurate solutions using reduced chemical kinetic models: a new model reduction method for models rigorously validated over ranges," Combust. Theor. Model., Vol. 11, No. 1, pp. 127–146.

[18] K. He, M.G. Ierapetritou, I.P. Androulakis, 2008, "A graph-based approach to developing adaptive representations of complex reaction mechanisms," Combust. Flame, Vol. 155, No. 4, pp. 585–604.

[19] T. Lu, C.K. Law, 2005, "A directed relation graph method for mechanism reduction," Proc. Combust. Inst. 30 (2005) 1333–1341.

[20] X.L. Zheng, T. Lu, C.K. Law, 2007, "Experimental counterflow ignition temperatures and reaction mechanisms of 1,3-butadiene," Proc. Combust. Inst. 31 (2007) 367–375.

[21] T. Lu, C.K. Law, 2008, "Strategies for mechanism reduction for large hydrocarbons: n-heptane," Combust. Flame, Vol. 154, pp.153–163.

[22] P. Pepiot-Desjardins, H. Pitsch, 2008, "An efficient error-propagation-based reduction method for large chemical kinetic mechanisms," Combust. Flame, Vol. 154, No. 1–2, pp. 67–81.

[23] W. Sun, Z. Chen, X. Gou, Y. Ju, 2010, "A path flux analysis method for the reduction of detailed chemical kinetic mechanisms," Combust. Flame, Vol. 157, pp. 1298–1307.

[24] K.E. Niemeyer, C.-J. Sung, M.P. Raju, 2010, "Skeletal mechanism generation for surrogate fuels using directed relation graph with error propagation and sensitivity analysis," Combustion and Flame, Vol. 157, No. 9, pp. 1760–1770.

[25] T. Lu, P. Max, Z. Luo, S.M. Sarathy, W.J. Pitz, S. Som, and D.E. Longman, 'Directed relation graph with expert knowledge for skeletal mechanism reduction', in *7th US National Combustion Meeting*, Atlanta, GA, 2011.

[26] Z. Luo, M. Plomer, T. Lu, S. Som, D.E. Longman, "A reduced mechanism for biodiesel surrogates with low temperature chemistry," *7th US National Combustion Institute Meeting*, Atlanta, March 2011.

[27] S. Som, D.E. Longman, Z. Luo, M. Plomer, T. Lu, "Three Dimensional simulations of diesel sprays using n-dodecane as a surrogate," *Eastern States Section of the Combustion Institute Fall Technical Meeting*, Storrs, October 2011.

[28] P.K. Senecal, K.J. Richards, E. Pomraning, T. Yang, M.Z. Dai, R.M. McDavid, M.A. Patterson, S. Hou, T. Sethaji, 2007, "A new parallel cut-cell Cartesian CFD code for rapid grid generation applied to in-cylinder diesel engine simulations," SAE Paper No. 2007-01-0159.

[29] K.J. Richards, P.K. Senecal, E. Pomraning, 2008, CONVERGE (Version 1.3) Manual, Convergent Science, Inc., Middleton, WI.

[30] Aceves, S. M. Flowers, D. L., Westbrook, C., Smith, J. et al., "A Multi-Zone Model for Prediction of HCCI Combustion and Emissions," SAE Technical Paper 2000-01-0327.

[31] Flowers, D., Aceves, S., Smith, R., Torres, J., Girard, J., and Dibble, R. 2000. HCCI in a CFR engine: Experiments and detailed kinetic modeling. SAE paper 2000-01-0328.

[32] A Babajimopoulos,D N Assanis,D L Flowers,S M Aceves,R P Hessel "A fully coupled computational fluid

 Copyright © 2012 by ASME

dynamics and multi-zone model with detailed chemical kinetics for the simulation of premixed charge compression ignition engines", International Journal of Engine Research, October 1, 2005; vol. 6, 5: pp. 497-512.

[33] Hessel, R. P., Foster E. E.,Aceves, S. M,Davisson, M. L.,Espinosa-Loza, F.,Flowers, D. L., Pitz W. J.,Dec J. E.,Sjöberg, M.,Babajimopoulos, A., Modeling Iso-octane HCCI Using CFD with Multi-Zone Detailed Chemistry; Comparison to Detailed Speciation Data Over a Range of Lean Equivalence Ratios, SAE Technical Paper 2008-01-0047.

[34] Liang, L., Stevens, J., Farrell, J., "A Dynamic Multi-Zone Partitioning Scheme for Solving Detailed Chemical Kinetics in Reactive Flow Computations", Combustion Science and Technology, 181(11) 2009 1345-1371.

[35] Raju, M., Wang, M., Dai, M., Piggott, W., Flowers, D. "Acceleration of Detailed Chemical Kinetics Using Multi-zone Modeling for CFD in Internal Combustion Engine Simulations," SAE 2012-04-16.

[36] H.K. Ciezki, G. Adomeit, 1993, "Shock-tube investigation of self-ignition of n-heptane-air mixtures under engine relevant conditions," Vol. 93, No. 4, pp. 421-433.

[37] Minetti, R., Carlier, M., Ribaucour, M., Therssen, E., and Sochet, L. R., Combust. Flame 102:298–309 (1995).

[38] http://www.sandia.gov/ecn/

[39] L.M. Pickett, C.L. Genzale, G. Bruneaux, L.M. Malbec, L. Hermant, C. Christiansen, J. Schramm. Comparison of diesel spray combustion in different high-temperature, high-pressure facilities. *SAE Paper* (2010) 2010-01-2106.

[40] L.M. Pickett, J. Manin, C.L. Genzale, D.L. Sieber, M.P.B. Musculus, C.A. Idicheria. Relationship between diesel fuel spray vapor penetration/dispersion and local fuel mixture fraction. *SAE Paper* (2011) 2011-01-0686.

[41] Lu, T. F., Law, C.K., Yoo, C.S., Chen J.H., 2009, "Dynamic Stiffness Removal for Direct Numerical Simulations", Combustion and Flame, Vol. 156 (8), pp.1542-1551.

[42] S. Som, D.E. Longman, Z. Luo, M. Plomer, T. Lu, P.K. Senecal, E. Pomraning, "Simulating flame lift-off characteristics of diesel and biodiesel fuels using detailed chemical-kinetic mechanisms and LES turbulence model," ICEF2011-60051, *ASME Internal Combustion Engine Division Fall Technical Conference*, Morgantown, USA, October 2011.

Copyright © 2012 by ASME